

# Field-Effect Transistor with Graphene by Direct Alcohol CVD

Masahiro Ishii, Atsushi Nakamura, Hiroshi Inokawa\* and Jiro Temmyo

Research Institute of Electronics, Shizuoka University, 3-5-1 Johoku, Naka-ku, Hamamatsu 432-8011, Japan

Phone: +81-53-478-1308 \*E-mail: inokawa06@rie.shizuoka.ac.jp

## 1. Introduction

Recent observations have revealed that single- or few-layer graphene is very attractive as an electronic material due to its excellent transport characteristics [1]. In order to make it viable in real applications, many efforts have been done to produce large-area material with some success [2], [3]. However, most of the techniques still require transfer process from metallic substrate, which may degrade the productivity and quality as well. Therefore, it is worth while trying to deposit graphene directly on insulator substrate. Actually, Miyasaka, et al. successfully grew multi-layer graphene on a sapphire substrate without catalyst metal by alcohol chemical vapor deposition (CVD), and characterized it with physical analyses [4]. This time, by making field-effect transistors (FET), electrical characteristics of the graphene directly deposited on SiO<sub>2</sub> by alcohol CVD are investigated in detail.

## 2. Device Fabrication

FETs were fabricated using a special substrate with a built-in shadow mask [5] for source/drain metal (70-nm Au/30-nm Ni) evaporation. Figure 1(a) shows the plane view of the deposition mask. The sizes of the suspended mask ( $L$ ,  $W$ ) were varied to obtain various channel lengths and widths of the FET. Figure 1(b) shows the cross-sectional view of the FET. Prior to the evaporation of the metal, 0.7-nm-thick graphene was deposited with ethanol and Ar flow rates of 10 and 200 sccm at 10 Torr and 1000 °C. The thickness was evaluated by the spectroscopic reflectance using a 95-nm SiO<sub>2</sub>/Si monitor assuming the optical constants by Blake et al. [6]. Since the graphene CVD was conformal, the graphene on the top surface was removed by resist coating and blanket etching by oxygen plasma to attain electrical isolation. The substrate is used as the gate, and the gate oxide thickness is 20 nm.

## 3. Electrical Characterization

Figure 2 shows typical  $I_d$ - $V_g$  and  $I_d$ - $V_d$  characteristics. Since the slopes of the  $I_d$ - $V_g$  are always negative, the graphene only shows the hole conduction. Modulation range of the  $I_d$  is 19% for a  $V_g$  change from -4 to 4 V. This small change may be caused by the large shift of the Dirac point, and/or the leakage through the graphene on the sidewall of the spacer and the back side of the overhang.

Figure 3 shows drain resistance  $R_d$  ( $=V_d/I_d$ ) as a function of the effective  $L/W$ , which is calculated by Laplace equation for stationary current field to include the contribution of the current flowing outside of the  $L \times W$  area. At the in-

tersection of  $L/W=0$ , parasitic series resistances larger than those of the channel can be observed. These are comparable to the reported values of the contact resistance [7].

Figure 4 shows the transconductance  $G_m$  with respect to the effective  $L/W$ . Ideally,  $G_m$  should be inversely proportional to the  $L/W$ , but the effect of the  $L/W$  reduction saturates at small  $L/W$ 's. With a series resistance  $R_{sd}$ ,  $G_m$  in the linear region can be expressed as

$$G_m = \beta V_d / (1 + \beta R_{sd} V_{od})^2 \quad \text{and} \quad \beta = \mu C_{ox} W/L, \quad (1)$$

where  $V_{od}$ ,  $\mu$  and  $C_{ox}$  are gate voltage overdrive, mobility and gate capacitance, respectively. The experimental  $G_m$  can be explained well, if  $R_{sd}$ 's of 1.8 and 4.6 k $\Omega$  are assumed for  $W=4.0$  and  $0.4 \mu\text{m}$ , respectively.

Figure 5 shows the field-effect mobility with respect to the effective  $L/W$ . The raw mobility obtained by  $G_m L / (C_{ox} V_d W)$  shows unusual decreasing trend as the  $L/W$  is reduced, but the mobility corrected based on eq. (1) and the same  $R_{sd}$  is almost constant at around 15 cm<sup>2</sup>/Vs. This is much below that of a high-quality single-crystal graphene, but is appreciably high for a subnanometer-thick p-channel TFT material.

Figure 6 shows the temperature dependences of the  $R_d$  and  $G_m$ . The former decreases gradually as the temperature increases, and the latter is almost independent of the temperature. These temperature dependences are not like those of monolayer graphene or graphite, but rather similar to those of a few-layer graphene [8].

## 4. Conclusions

We investigated the field effect of subnanometer-thick graphene directly grown by alcohol CVD. It showed only the hole conduction with a mobility of about 15 cm<sup>2</sup>/Vs. The  $R_d$  increased slightly as the temperature went down from 300 to 50 K, and the  $G_m$  was almost independent of the temperature, which is rather similar to the behavior of a few-layer single-crystal graphene. The capability of the large-area direct deposition would be of great use, if the transport properties were improved.

## References

- [1] A. K. Geim and K. S. Novoselov, *Nature Mat.* **6** (2007) 183.
- [2] X. Li, W. Cai, J. An, S. Kim, J. Nah, D. Yang, R. Piner, A. Velamakanni, I. Jung, et al., *Science* **324** (2009) 1312.
- [3] Z. Sun, Z. Yan, J. Yao, E. Beitler, Y. Zhu and J. M. Tour, *Nature* **468** (2010) 549.
- [4] Y. Miyasaka, A. Nakamura and J. Temmyo, *Jpn. J. Appl. Phys.* **50** (2011) 04DH12.
- [5] H. Inokawa, M. Nagase, S. Hirono, T. Goto, H. Yamaguchi and K. Torimitsu, *Jpn. J. Appl. Phys.* **46** (2007) 2615.

[6] P. Blake, E. W. Hill, A. H. C. Neto, K. S. Novoselov, D. Jiang, R. Yang, et al., *Appl. Phys. Lett.* **91** (2007) 063124.  
 [7] K. Nagashio, T. Nishimura, K. Kita and A. Toriumi, *Appl.*

*Phys. Lett.* **97** (2010) 143514.  
 [8] K. Nagashio, T. Nishimura, K. Kita and A. Toriumi, *Jpn. J. Appl. Phys.* **49** (2010) 051304.

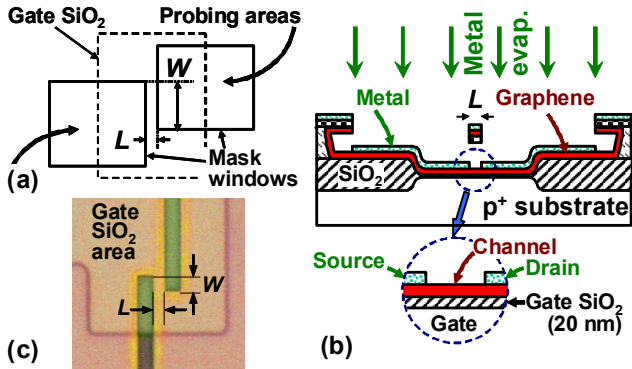


Fig. 1(a) Plane and (b) cross-sectional views of the graphene FET. (c) Optical micrograph of the sample before graphene CVD. Graphene on the top surface of the sample was removed by resist coating and blanket etching prior to the metal evaporation.

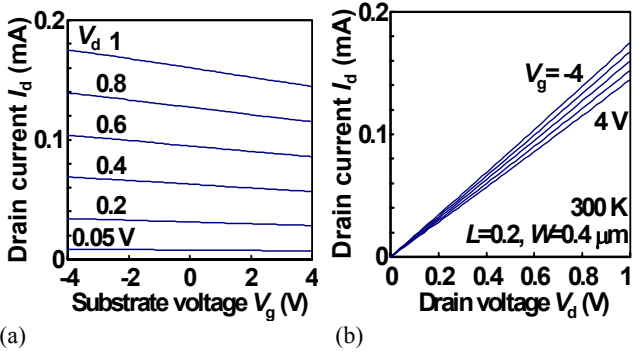


Fig. 2(a)  $I_d$ - $V_g$  characteristics and (b)  $I_d$ - $V_d$  characteristics of the graphene FET measured in vacuum at 300 K. Only the hole conduction can be observed under the present substrate (gate) bias condition. Modulation of the  $I_d$  by  $V_g$  of  $\pm 4$  V is 19%.

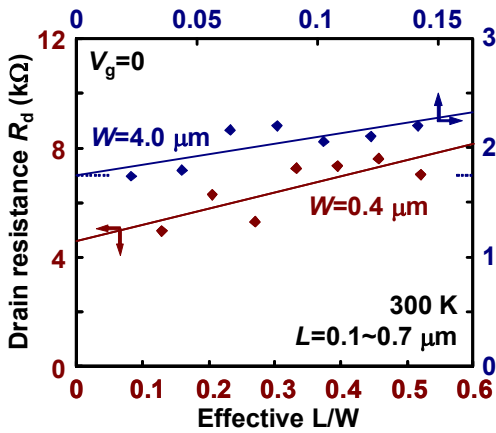


Fig. 3 Drain resistance  $R_d$  ( $=V_d/I_d$ ) as a function of effective  $L/W$  for the channel widths of 0.4 and 4.0  $\mu\text{m}$ . Effective  $L/W$  is obtained by solving Laplace equation to compensate for the geometrical effect due to the absence of graphene isolation etch. Large series resistance can be observed.

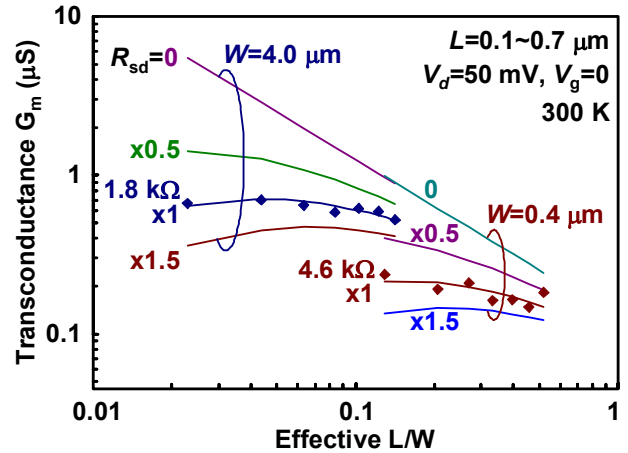


Fig. 4 Transconductance  $G_m$  as a function of effective  $L/W$ . Experimental data can be explained well by taking the effect of parasitic series resistance  $R_{sd}$  into account.

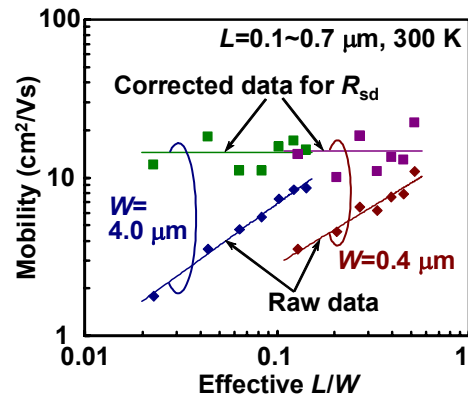


Fig. 5 Field-effect mobility as a function of effective  $L/W$ . After the correction for series resistance  $R_{sd}$ , mobilities become nearly constant at around  $15 \text{ cm}^2/\text{Vs}$ .

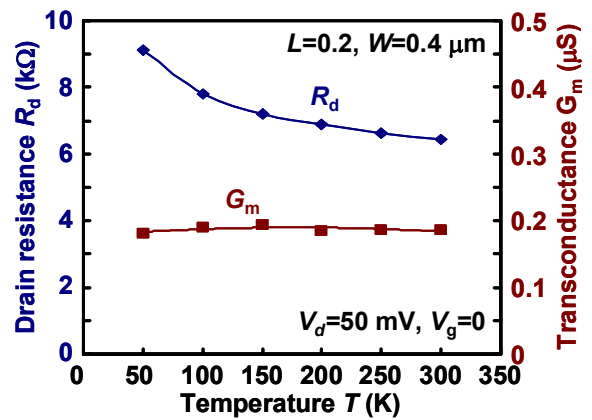


Fig. 6 Temperature dependences of the  $R_d$  and  $G_m$ . The dependences are not like those of monolayer graphene or graphite, but rather similar to those of a few-layer graphene [8].